

RESEARCH ARTICLE

Performance Analysis of Brushless Wound Rotor Vernier Machine by Utilizing Third Harmonic Field Excitation

SHEIKH YASIR HAMMAD¹, JUNAID IKRAM¹, RABIAH BADAR¹,
SYED SABIR HUSSAIN BUKHARI², (Senior Member, IEEE),
LAIQ KHAN¹, AND JONGSUK RO^{3,4}

¹Department of Electrical and Computer Engineering, COMSATS University Islamabad, Islamabad 44000, Pakistan

²Department of Electrical Engineering, Sukkur IBA University, Sukkur, Sindh 65200, Pakistan

³School of Electrical and Electronics Engineering, Chung-Ang University, Seoul 06974, Republic of Korea

⁴Department of Intelligent Energy and Industry, Chung-Ang University, Seoul 06974, Republic of Korea

Corresponding author: Jongsuk Ro (jongsukro@gmail.com)


This work was supported in part by the National Research Foundation of Korea (NRF) Grant by the Korean Government through the Ministry of Science and ICT (MSIT) under Grant NRF-2022R1A2C2004874; in part by the Korea Institute of Energy Technology Evaluation and Planning (KETEP) and the Ministry of Trade, Industry and Energy (MOTIE), Republic of Korea, under Grant 20214000000280; in part by the Chung-Ang University Research Grant, in 2022; and in part by the Brain Pool (BP) Program by the Ministry of Science and ICT through the NRF under Grant 2019H1D3A1A01102988.

ABSTRACT In this paper, a self-excited topology by utilizing third harmonic field excitation is proposed for realizing the brushless operation of the Wound Rotor Vernier Machine (WRVM). The proposed topology consists of two windings housed inside the stator periphery connected in series with the three-phase diode rectifier. The two windings on the stator periphery are the 12-pole excitation and 4-pole armature winding. The 12-pole excitation winding is linked to the open-end star winding of 4-pole armature winding with the help of a three-phase diode rectifier. When the current is supplied by the inverter, a 4-pole, and a 12-pole Magneto Motive Force (MMF) is developed in the machine air gap. The 4-pole fundamental MMF component develops the main stator field and a 12-pole MMF component develops the third harmonic field. The third harmonic field tends to induce a harmonic current in the harmonic winding which is housed inside the rotor periphery. The induced harmonic current is then rectified by the means of an H-bridge rectifier to excite the rotor field winding, and this realizes the brushless operation of a WRVM. The Two-dimensional Finite Element Analysis (2D-FEA) is carried out in a JMAG designer software to validate the operation of the proposed BL-WRVM. Furthermore, the proposed topology is analyzed for the comparative analysis with the sub-harmonic model after the verification of FEA results. The comparative analysis shows that the third harmonic topology results in improved average torque when compared to the subharmonic wound-rotor vernier machine.

INDEX TERMS Wound rotor synchronous machines, brushless operation, single-inverter-fed, harmonic field excitation, third harmonic excitation, wound rotor vernier machine.

I. INTRODUCTION

The development of electric machines has grown significantly over the past century in a wide range of industrial applications, such as electric automobiles, wind turbines, ship

The associate editor coordinating the review of this manuscript and approving it for publication was Alfeu J. Sguarezi Filho .

propulsion systems, and in robotics [1]. On the installation of high-energy density Permanent Magnet (PM) materials, the PM machine provides superior performance and hence they become very attractive in high-performance applications. Similarly, the PM-assisted (PM-a) machines are the other candidate that pursued the researchers to improve the efficiency of a machine. The PMs are positioned on the

TABLE 1. Segregation of different machine topologies.

Brushless Machines	Achievements	Limitations
(PM-assisted) Novel Wound Field Synchronous Machine	<ul style="list-style-type: none"> ❖ No use of slip-rings and brushes ❖ Efficiency is high 	<ul style="list-style-type: none"> ❖ Torque density is reduced due to PM ❖ Optimal design for pole head shape is required
Brushless Synchronous Machine With Additional Harmonic Field Windings	<ul style="list-style-type: none"> ❖ No use of PM, by adding excitation winding brushless operation is achieved 	<ul style="list-style-type: none"> ❖ Power density reduces due to the large volume of a stator
Dual Inverter Subharmonic BL-WRSM	<ul style="list-style-type: none"> ❖ Subharmonic component is generated by distributing armature windings into two halves 	<ul style="list-style-type: none"> ❖ Two inverters are necessary ❖ High torque ripple ❖ Copper loss increased
BL-WRSM with Zero-Sequence Third-Harmonic Field Excitation	<ul style="list-style-type: none"> ❖ Additional harmonics reduced ❖ Torque density was improved compared to other machines 	<ul style="list-style-type: none"> ❖ Ripple increases due to switching loss ❖ Low efficiency as more current flows
Dual and single inverter fed BL-WRSM for Third-Harmonic Field Excitation	<ul style="list-style-type: none"> ❖ No need for extra switches ❖ Output torque was improved with low ripple rate 	<ul style="list-style-type: none"> ❖ Complex control scheme is used to generate third harmonic field excitation
Comparison of PMVM and PMSM	<ul style="list-style-type: none"> ❖ Average torque increased for PMVM as compared to PMSM due to different pole number 	<ul style="list-style-type: none"> ❖ PMs cause several disadvantages
Single and Dual Inverter Fed subharmonic BL-WRVM	<ul style="list-style-type: none"> ❖ Brushless operation also achieved ❖ Torque was slightly increased 	<ul style="list-style-type: none"> ❖ Unbalanced magnetic distribution

opening slots of the rotor to maximize the output torque [2]. However, the fluctuating supply of rare-Earth materials is increasing the cost of permanent magnets. Furthermore, when taking a close look at industries for the supply of rare-earth materials, one concludes a drastic impact on environmental problems [3].

The Wound Rotor Synchronous Machine (WRSM), in which the DC is supplied to the field winding with the help of slip rings and carbon brushes is known as a brushed machine. The slip rings and carbon brushes contact each other to provide excitation to the field winding. The continuous sparking of these mechanical structures generates heat, which makes them necessary to replace and this reduces the efficiency and reliability of the machine [4]. Similarly, an additional exciter expands the system's size and expense. Thus, such types of motors should never be utilized for an operation that demands for long life and reliability. The main goal is to develop a machine to enhance the field winding without PMs, carbon brushes and slip rings [5].

The self-excited machines are the fresh candidates providing better performance for the excitation to the rotor field winding. The significant question that arises, is how to realize the brushless operation of a wound rotor machine without conventional exciters. Nonetheless, harmonic excitation could be a viable solution to operate a machine in brushless mode. Harmonic excitation mainly refers to the sub-harmonic component and third-harmonic component [6]. A useful power could be achieved by harmonic field excitation to energize the rotor field winding [7]. An additional harmonic component along with the fundamental component is generated to obtain the Magneto Motive Force (MMF) in the machine air gap. Through this mechanism, voltage is

induced in the harmonic winding that is housed inside the rotor periphery.

Several researchers have proposed different harmonic techniques to achieve the brushless operation of WRSMs. These methods are divided into two categories 1) space harmonics and time harmonics [8]. An additional harmonic winding along with the armature winding is equipped in the stator slots proposed in [9]. Two windings with equal pole pairs were housed inside the stator periphery namely armature winding and additional harmonic winding. This topology creates a third harmonic and fundamental component, inducing a bipolar-induced voltage in 12-pole rotor harmonic winding that supplies a rectified current to the field winding. The power density of the machine was reduced due to the large volume of the stator. This type of brushless scheme is not suitable for industrial applications due to losses produced by other components [10].

It was realized that a conventional power source or inverter would be sufficient for the brushless operation of the WRSM instead of installed devices on the stator periphery. Hence, a dual-inverter-based prototype was configured [11]. The proposed work shows the scheme by distributing the armature windings in two equal halves with separate star-connection mounted in the stator periphery. Both these windings were connected with two separate inverters supplying different current magnitudes. This type of arrangement will generate sub-harmonic and fundamental components in the machine air gap. This will then induce an Electromotive Force (EMF) in the 2-pole excitation winding which is housed inside the rotor. The induced voltage is then rectified to energize the field winding. The difference in current magnitudes resulting in higher torque ripple and reduces the torque density of a machine. However, by utilizing subharmonic components,

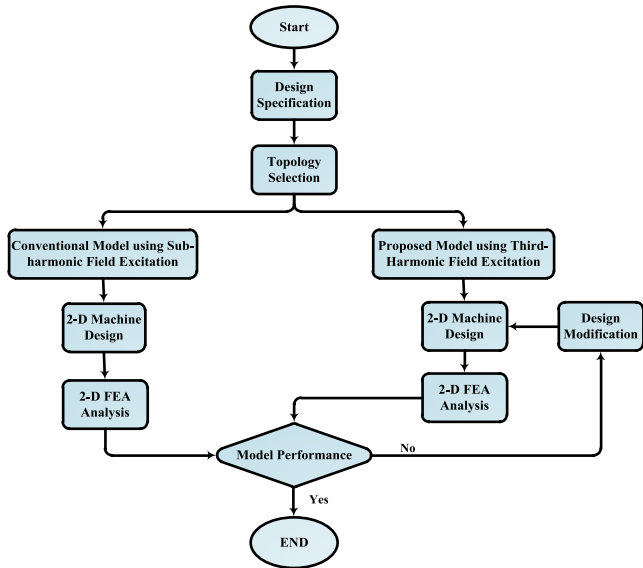


FIGURE 1. Flow of research process.

these topologies suffer from low average output torque due to underrated current in the harmonic winding.

Hence, to improve the output torque, a scheme is designed with additional six-thyristor switches arranged in antiparallel combination was introduced for generating time harmonics in the air gap field [12]. The operation of these switches creates both the fundamental as well as third harmonic components to generate the required MMF. This induces the harmonic voltage in the rotary harmonic winding. Afterward, the bridge rectifier converts this induced voltage and feeds to the rotor field winding. The rotor field gets link with the main field because of the equal number of poles, realizing the brushless operation of WRSM by using thyristors. However, this topology results in low efficiency due to the additional switching losses installed in the armature winding. Furthermore, this topology also results in high torque ripple which increases the noise and reduced the life of the machine.

Synchronous machine require larger size and heavy weight for the low-speed applications. Consequently, geared systems provides a solution to drive a system at low speed comprising high transmission torque. Friction loss, vibrations that cause noise, and heat production are the main limitations subjected to the traditional mechanical gears system. Furthermore, these require regular lubrication for smooth operation otherwise they may be jammed. Apart from this, Magnetic Gears (MGs) were developed to overcome the issues related to mechanical gears.

The concept of the Vernier Machine (VM) was first proposed by C.H. Lee proposed that uses the magnetic gearing phenomenon caused by flux modulation to generate high torque at a low speed [13]. These machines achieve high torque due to increased rotor poles. Moreover, it is not necessary to employ any mechanical gear system with a vernier machine. In comparison to the vernier machine, the syn-

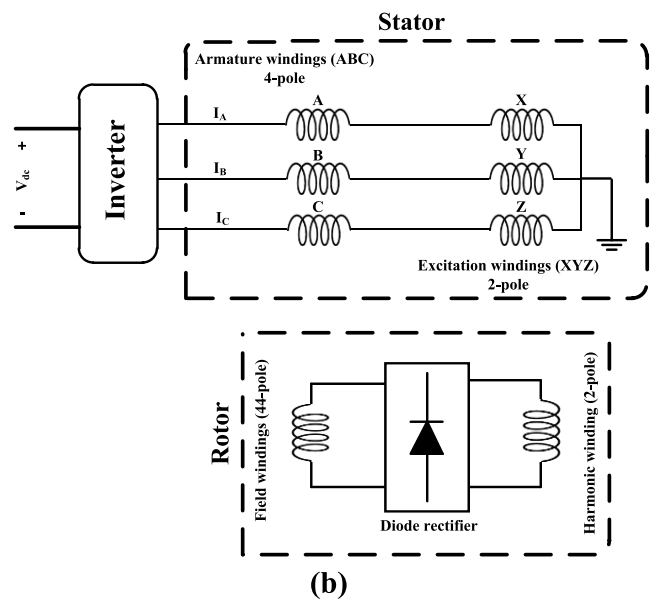
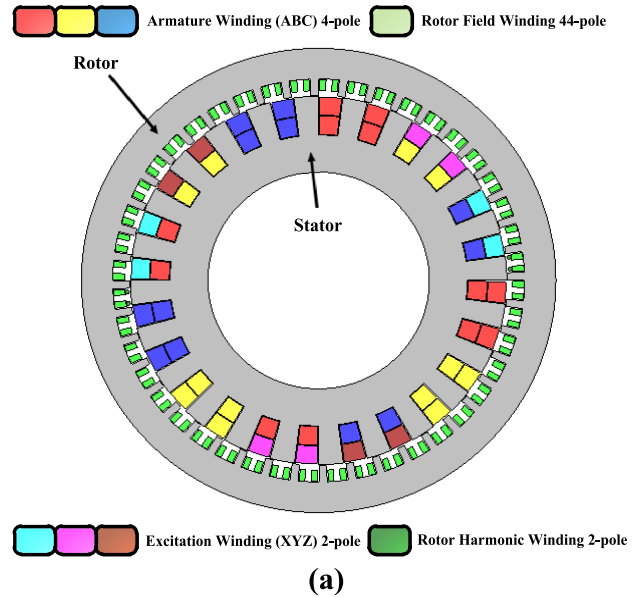


FIGURE 2. (a) 2D design of subharmonic BL-WRVM (b) Schematic representation of subharmonic BL-WRVM.

chronous machine operates with an equal number of poles as that of the stator and rotor. Whereas in VM, the rotor and stator poles are different from each other.

Due to advancements in permanent magnet technology, Permanent Magnet VMs (PMVMs) have attracted a lot of attention in recent years. PMVMs seemed as a crucial potential candidate for applications such as ship propulsion and wind power generation [14], [15]. Due to various consequences related to PMs and brushed WRSMs, the Brushless Wound Rotor Vernier Machine (BL-WRVM) was developed by splitting the armature winding into two halves [16]. This topology contains two inverters supplying different current magnitudes to the armature winding. This generates a

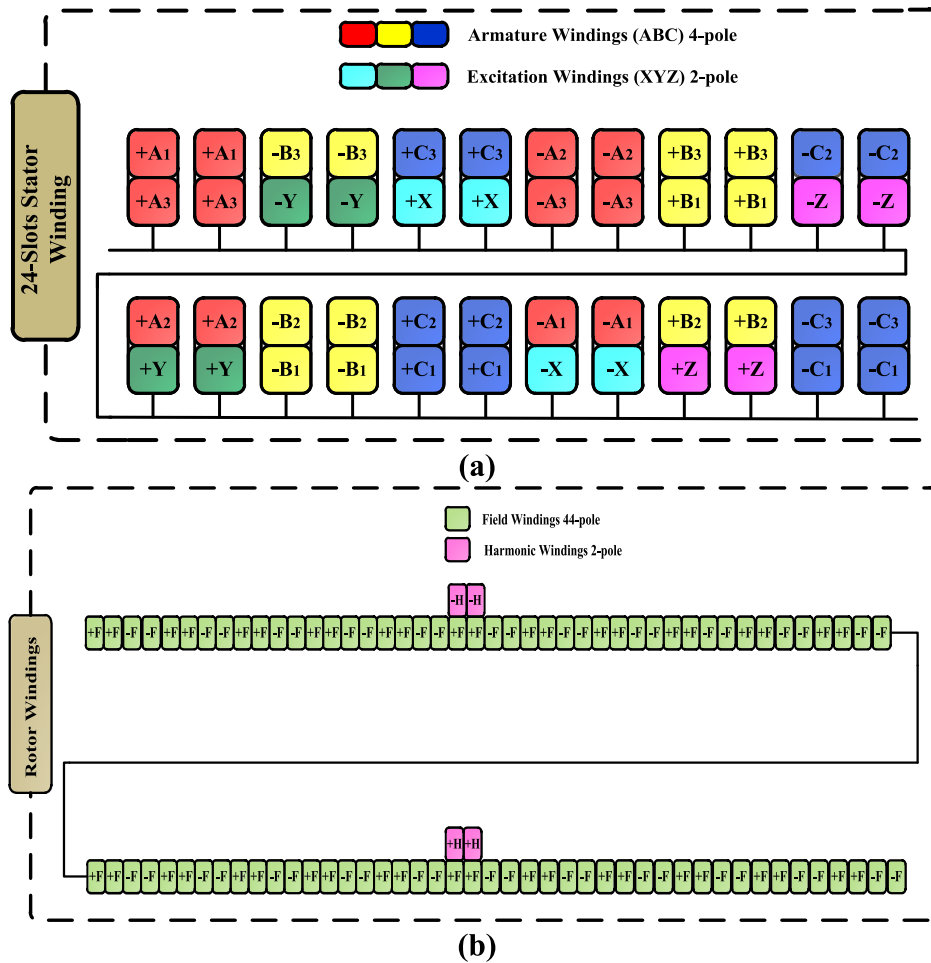


FIGURE 3. Winding layout for subharmonic BL-WRVM (a) Stator windings (b) Rotor windings.

sub-harmonic component in the machine air gap along with the fundamental component.

A single inverter-fed topology of BL-WRVM with an additional winding (XYZ) was equipped in series with the three-phase armature winding (ABC) [17]. This generates the required MMF to induce the voltage in rotor harmonic winding. This induced voltage feeds to the field winding after rectification and that realizes the brushless operation of WRVM. Based on the above arrangement, another work was done in [18] to operate a WRSM in a brushless mode. This topology was equipped with the single-phase 2-pole winding (X) instead of the three-phase (XYZ) winding fastened with the armature winding to obtain the air-gap MMF for brushless operation. A similar approach was done with the WRVM in order to improve the torque performance [19]. In this approach, the two-pole excitation winding contains three coils that were distributed among six slots. Whereas the four-pole armature winding is distributed to 18 slots. The topology is the same as in [18] but implemented in vernier machine to enhance its torque performance. Table 1 summarizes different types of machine topologies with their achievements and limitations.

The WRVMs topologies are implemented to obtain the brushless operation by using subharmonic field excitation. This research exhibits the brushless operation of WRVM by utilizing third-harmonic field excitation. In the proposed brushless-vernier machine, stator slots contain three-phase armature winding, a single-phase excitation winding along with a three-phase diode rectifier. This develops a four-pole and twelve-pole MMF in the air gap. On the other hand, the rotor slots are wound with harmonic and field windings having twelve-pole and forty-four-pole. Two-dimensional Finite Element Analysis (2D-FEA) is carried out to validate the operation of the proposed BL-WRVM. Furthermore, the proposed topology is analyzed for the comparative analysis with the sub-harmonic model after the verification of FEA results. The results show that the average torque and field current is enhanced while the torque ripple of a machine is reduced with the third harmonic excited BLWRVM. The research methodology of the proposed work is conveyed in Fig. 1.

The manuscript is divided into six sections. In the first section, a brief introduction about PM machines and brushless machines with different topologies was presented. Sec-

TABLE 2. Design specifications for conventional & proposed model of the brushless wound rotor vernier machine (BL-WRVM).

MACHINE ATTRIBUTES	Units	Conventional Model	Proposed Model
ABC winding Poles	-	4	4
Excitation winding Poles	-	2	12
Excitation winding Coils	-	6	12
Stator inner diameter	mm	140	140
Stator outer diameter	mm	238	238
Stator armature winding turns (ABC)	turns/slot	90	90
Stator winding turns (XYZ)	turns/slot	90	-
Stator excitation winding turns (X)	turns/slot	-	45
Rotor field winding turns	turns/slot	36	36
Rotor harmonic winding turns	turns/slot	8	8
Rotor field poles	-	44	44
Rotor slots	-	44	44
Rotor inner diameter	mm	239	239
Rotor outer diameter	mm	300	300
Harmonic winding turns	turns/slot	8	8
air Gap Length	mm	0.5	0.5
Stack length	mm	30	30
Speed	rpm	300	300
Current	A (rms)	2.12	2.12
Slot fill factor	\hat{a}	0.79	0.79

tions II and III explain the brushless operation of WRVMs by subharmonic and third harmonic excitation whereas the working principle of a proposed BL-WRVM is explained in section IV. The comparison of electromagnetic performance between conventional and proposed topology is accounted in section V. After briefing these sections, a conclusion is made in section VI illustrating the comparative analysis between conventional and the proposed brush-less WRVM topologies.

II. CONVENTIONAL SUB-HARMONIC TOPOLOGY

The 2D model and schematic representation of a conventional subharmonic BL-WRVM is given in Fig.2 (a) and (b) [17]. It contains two sets of windings (armature & excitation) associated in series with each other having the same number of turns but with different pole-pairs. The armature windings (ABC) are wound to develop a 4-pole field whereas the excitation windings (XYZ) are wound to develop a 2-pole field that generates the subharmonic component to interact with the rotary harmonic winding. The induced harmonic current energizes the 44-pole field winding. The winding layout for the stator and rotor structure are given in Fig.3. (a) and (b) respectively.

III. PROPOSED THIRD HARMONIC TOPOLOGY

The proposed topology contains an open-winding star connection having three-phase armature winding (ABC) coupled in series with a single-phase excitation winding (X). The armature winding has 4-pole whereas the excitation winding

is having poles equal to three times the armature poles in order to generate third-harmonic excitation. A three-phase diode rectifier is fastened between these two windings. Figure. 4 (a) and (b) represents the 2D design and schematic representation of the proposed third harmonic BL-WRVM. The inverter supplies the current to the main winding, a 12-pole pulsating third-harmonic field is established in the air gap along with the 4-pole field. This originates an EMF in the rotor harmonic winding and supplies the rectified voltage to the rotor field winding. The rotor field winding after linking to the main armature winding realizes the brushless operation of the proposed BL-WRVM.

A. GEOMETRICAL AND STRUCTURAL DESIGN OF PROPOSED BL-WRVM

The design parameters for the 2-D model of BL-WRVM are presented in Table 2 [17] with the rotor harmonic winding modified to develop a 12-pole. The stator winding of the proposed machine is fabricated with a three-layered configuration. Table 2 shows that the number of turns of winding (X) for the proposed BL-WRVM is kept at half as compared to the conventional BL-WRVM as more coils are added in the proposed BL-WRVM in order to develop third-harmonic MMF. However, the overall number of turns for both machines is kept the same. The winding placement for the stator and rotor structure of a proposed BL-WRVM is highlighted in Fig.5. (a) and (b) respectively. The stator is comprised of 24 slots of three-layer outlet in which the two-layers are completely

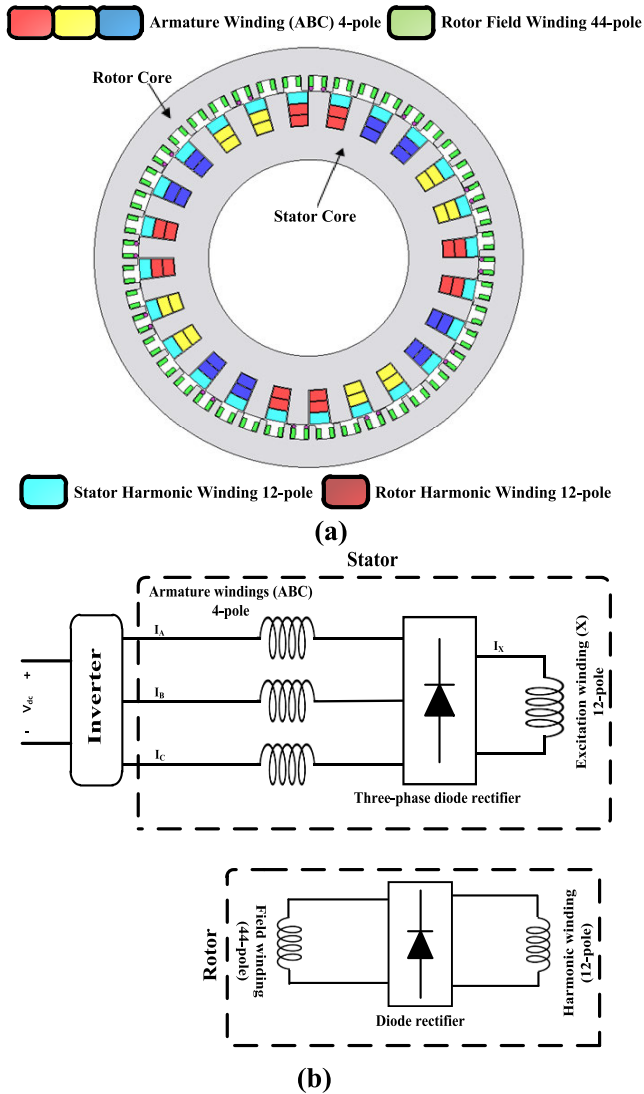


FIGURE 4. (a) 2D design of proposed third-harmonic BL-WRVM (b) Schematic representation of a proposed third-harmonic BL-WRVM.

filled with 4-pole armature windings (ABC) generating fundamental components. Whereas the excitation winding (X) occupies the third layer to create 12-poles for generating a third-harmonic component.

B. WORKING PRINCIPLE OF THIRD HARMONIC BL-WRVM TOPOLOGY

The inverter supplies a current (i_{abc}) to the armature winding is given in eq. (1).

$$\begin{aligned} i_a &= I_p \sin \omega_e t \\ i_b &= I_p \sin \left(\omega_e t - \frac{2\pi}{3} \right) \\ i_c &= I_p \sin \left(\omega_e t + \frac{2\pi}{3} \right) \end{aligned} \quad (1)$$

where ω denotes the rotor angular speed and I_p as the peak current.

The MMF developed by the stator field current is shown in eq. (2).

$$\begin{aligned} F_a &= i_a N_\phi [\sin \theta_e] \\ F_b &= i_b N_\phi \left[\sin \left(\theta_e - \frac{2\pi}{2} \right) \right] \\ F_c &= i_c N_\phi \left[\sin \left(\theta_e + \frac{2\pi}{2} \right) \right] \end{aligned} \quad (2)$$

where θ_e is the electrical angle and N_ϕ is denoted as the number of turns per phase for ABC winding. The four-pole armature MMF develops the main fundamental component and a twelve-pole harmonic MMF will generate the third-harmonic component which is pulsating harmonic field.

$$F = \frac{3N_\phi}{2} I_p \cos(\omega t - \theta_e) + I_x N_e \cos 3(\theta_e) \quad (3)$$

The above equation shows the overall MMF generated in the air gap, where F represents the MMF across the air gap, N_e represents the per-phase turns of winding (X), and the excitation current is represented by I_x [18].

The harmonic and the field windings are present in the rotor periphery attached in series with the rectifier. Both of these windings are designed for different poles. Rotor's harmonic winding is made of twelve-pole, whereas the field winding is made of forty-four-poles. A proper pole combination for the armature and field winding is chosen to operate a machine under vernier mode. Hence, for a vernier machine, the following equation must be satisfied.

$$p_r = Q_s \pm p_s \quad (4)$$

where p_r is the pole-pairs of the rotor field winding, Q_s is the number of stator slots, and p_s is the pole-pairs stator slots.

The rotor harmonic winding has equal poles to that of stator excitation winding through which they interact with each other and induce current which then feeds to the rotor field winding for its energization.

The proposed model has a 24-slot 4-poles for the stator and 44-poles for the rotor which is selected to satisfy the above equation. According to equation (4), the rotor poles differ from the stator poles by which their speed is different. Hence, the speed of the Vernier machine could be calculated by using the following expression [20], [21].

$$\frac{\omega_r}{\omega_{MMF}} = \frac{\text{Rotor speed}}{\text{Stator field speed}} = \frac{P_s}{P_r} \quad (5)$$

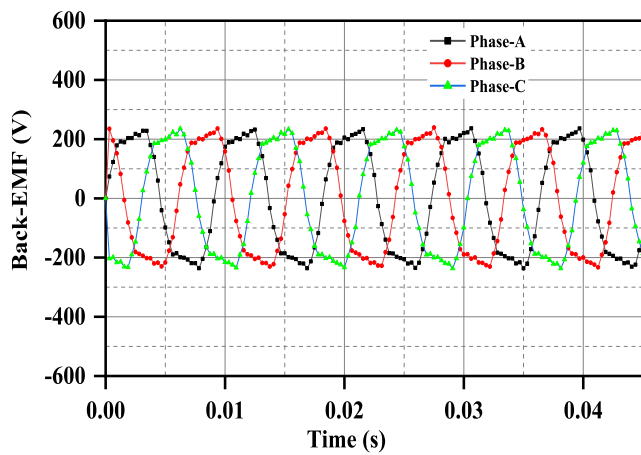
where ω_{MMF} is the main stator field speed and ω_r is the rotor speed.

IV. COMPARATIVE ANALYSIS OF ELECTROMAGNETIC PARAMETER

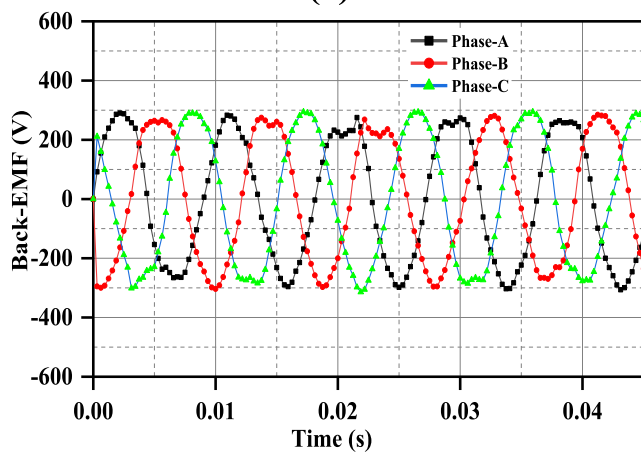
The 2-D FEA analysis of a proposed BL-WRVM with third-harmonic field excitation is carried out on the JMAG Designer to validate the performance analysis. Figure. 2 & 4 show the schematic design of the subharmonic and third harmonic model that utilizes a 24s44p outer rotor machine. An outer-rotor vernier machine is typically used because

TABLE 3. Quantitative results of conventional and proposed model.

Parameter	Units	Conventional Model	Proposed Model
Average Torque	Nm	38.04	41.91
Torque Ripple	%	30.18	49
Field Current	A	21.31	20.55
Excitation Current (XYZ)	A (rms)	2.12	-
Excitation Current (X)	A (rms)	-	6.34
Total Losses	W	117.11	121
Output Power	W	1473.93	1661.84
Efficiency	%	91.98	93.21
Power Factor	-	0.83	0.80



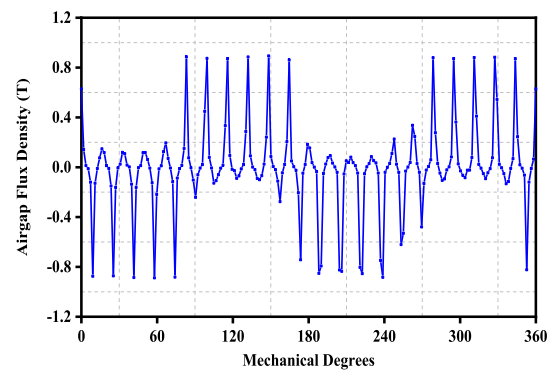
(a)



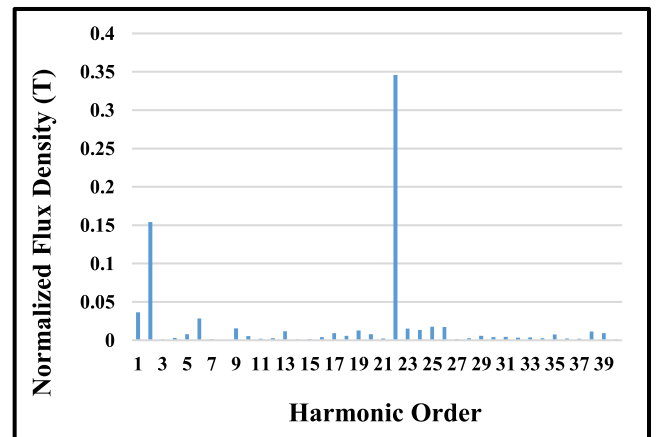
(b)

FIGURE 6. No-load Back-EMF of (a) Conventional model (b) Proposed model.

the Vernier principle as given in equation (4). The diode rectifier is also fitted inside the rotor structure which rectifies



(a)



(b)

FIGURE 7. No-load graphs of proposed model (a) Air-gap flux density (b) Harmonic order.

the harmonic current to energize the rotor field winding. Figure.12 (a) and (b) represent the induced harmonic current and the rectified field current of subharmonic and proposed third harmonic topology. It can be seen that the induced harmonic current is well linked with the field current for the proposed brushless topology. The average field current of the

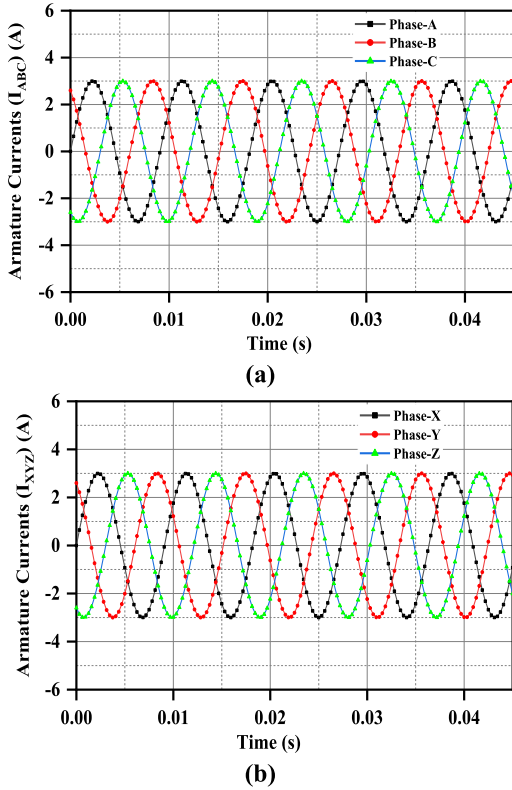


FIGURE 8. Armature currents of subharmonic BL-WRVM (a) ABC winding (b) XYZ winding.

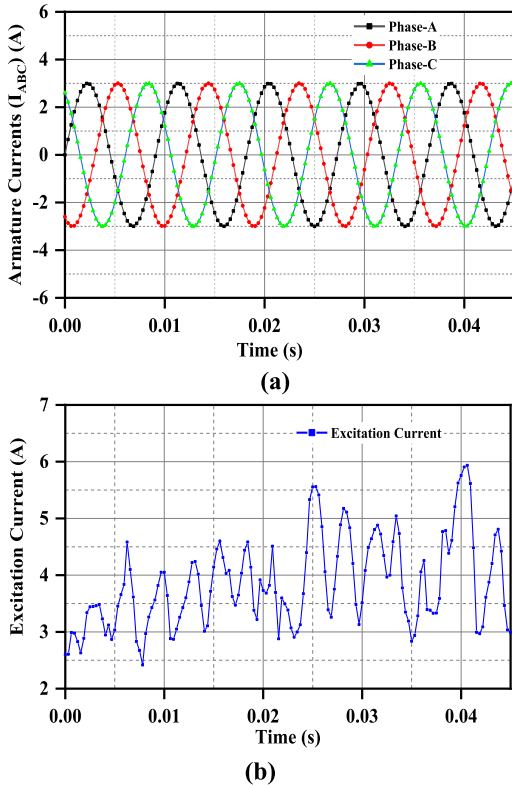


FIGURE 9. Armature currents of proposed third-harmonic BL-WRVM (a) ABC winding (I_{ABC}) (b) X winding (I_X).

proposed topology is about 20.55 A whereas the average field current for the conventional topology is 21.31 A. Due to low

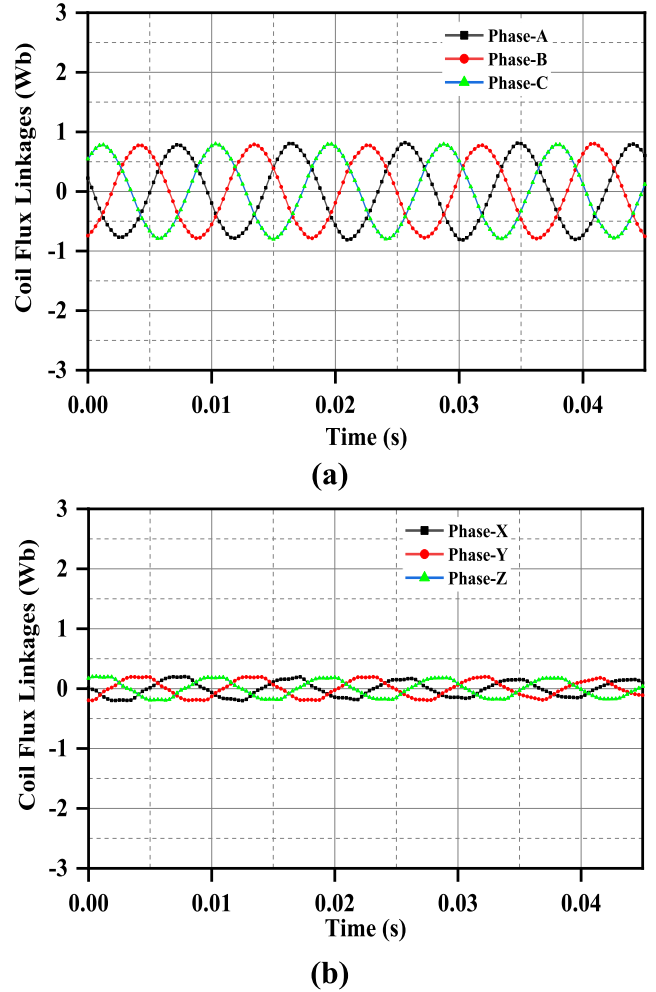


FIGURE 10. Coil flux linkages of subharmonic BL-WRVM (a) windings ABC (b) windings XYZ.

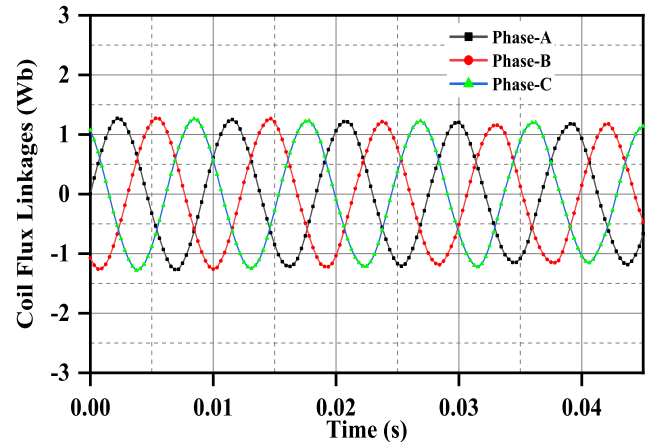
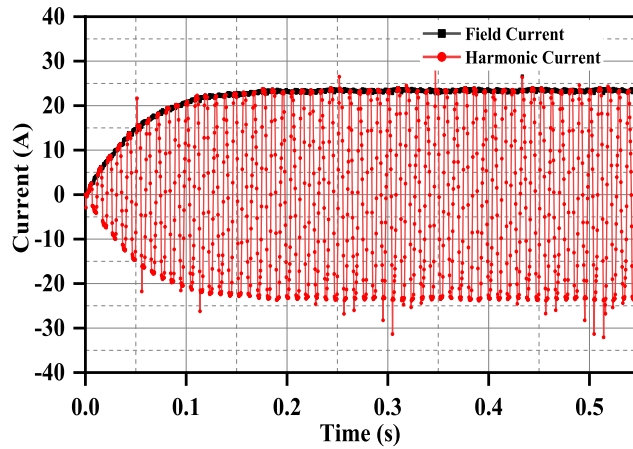


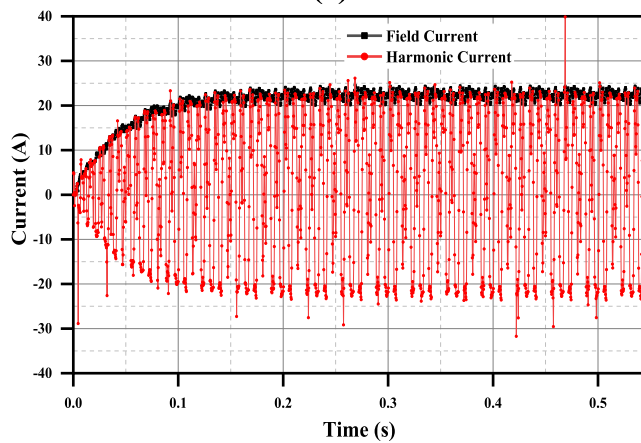
FIGURE 11. Coil flux linkages of proposed third-harmonic BL-WRVM ABC windings.

field current, the copper loss of the proposed topology will be less as compared to the conventional topology,

The output torque for the conventional topology is presented in Fig.13 (a). This shows that 38.04 Nm of average torque was generated by the subharmonic excitation with a torque ripple of 30.18% in a steady-state condition. On the



(a)

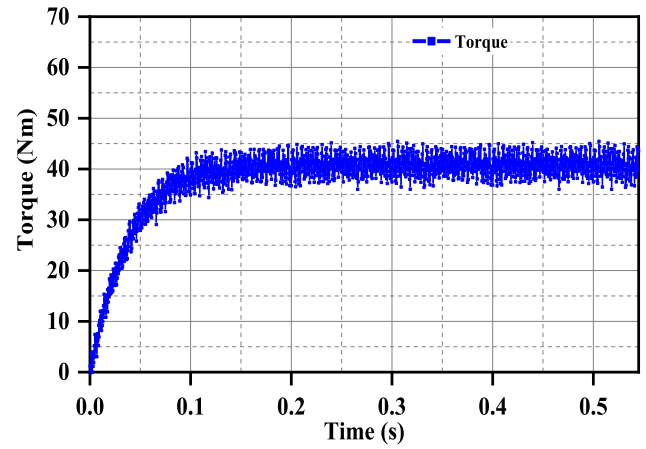


(b)

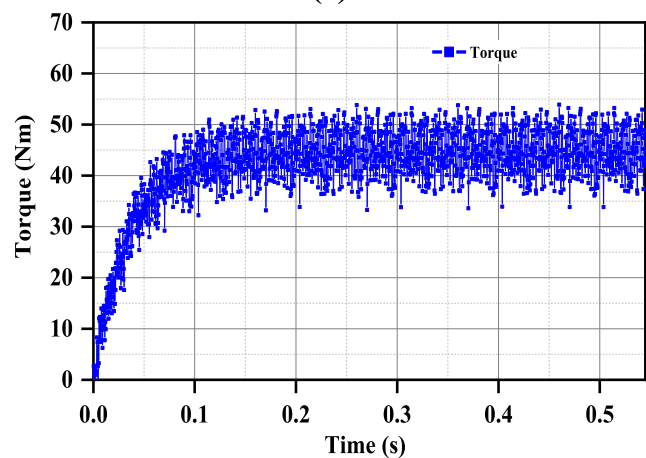
FIGURE 12. Harmonic and field currents of (a) subharmonic BL-WRVM (b) proposed third-harmonic BL-WRVM.

other hand, in Fig. 13 (b) 41.91 Nm of average output for the proposed third harmonic topology was generated with 49% ripples. The increase in torque ripple is due to a three-layer design in stator slots that is added for placing excitation winding. The comparative analysis shows better results related to the third-harmonic excitation model compared to the sub-harmonic excitation model and the results are shown in Table 3. Moreover, the total loss of both machines has been given in table 3 which shows that the proposed brushless topology exhibits 121W of a total loss whereas the total loss of conventional brushless topology is 117.11W. The total loss of proposed brushless topology is slightly higher than that of the conventional due to increased number of coils for third harmonic excitation. Similarly, the output power of conventional topology and proposed topology is 1473.98W and 1661.93W respectively and their efficiency is calculated as 92.98% and 93.21%.

Figure 14 (a) and (b) represent the flux density distribution plot for both harmonic excitation topologies are presented respectively. The distribution plot for the proposed third harmonic BL-WRVM is uniformly distributed along the stator and rotor side as compared to the subharmonic BL-WRVM.



(a)



(b)

FIGURE 13. Output torque of (a) subharmonic BL-WRVM (b) proposed third-harmonic BL-WRVM.

However, both machines exhibit saturation with flux density values lower than 2T.

V. CONCLUSION

In this paper, a simplified brushless operation of a self-excited wound-rotor vernier machine was analyzed with third harmonic field excitation. The proposed topology uses three-phase 4-pole (ABC) windings with a 12-pole single-phase (X) winding developing the main stator and third harmonic MMF components. This injects the third harmonic component into the 12-pole rotary harmonic winding and feeds the rectified current to excite the rotor field winding and realizes the brush-less operation of the proposed BLWRVM.

The proposed open winding scheme is advantageous in terms of inverter and excitation winding. It is based on a single inverter-fed topology that supplies current to the three-phase windings (ABC) and a single-phase winding (X) utilizing the third harmonic excitation. This simplifies the structure compared to the conventional one that uses three-phase (XYZ) for generating a subharmonic field.

Further, the finite element analysis was taken to ensure the performance analysis of BL-WRVM by the utilization of third

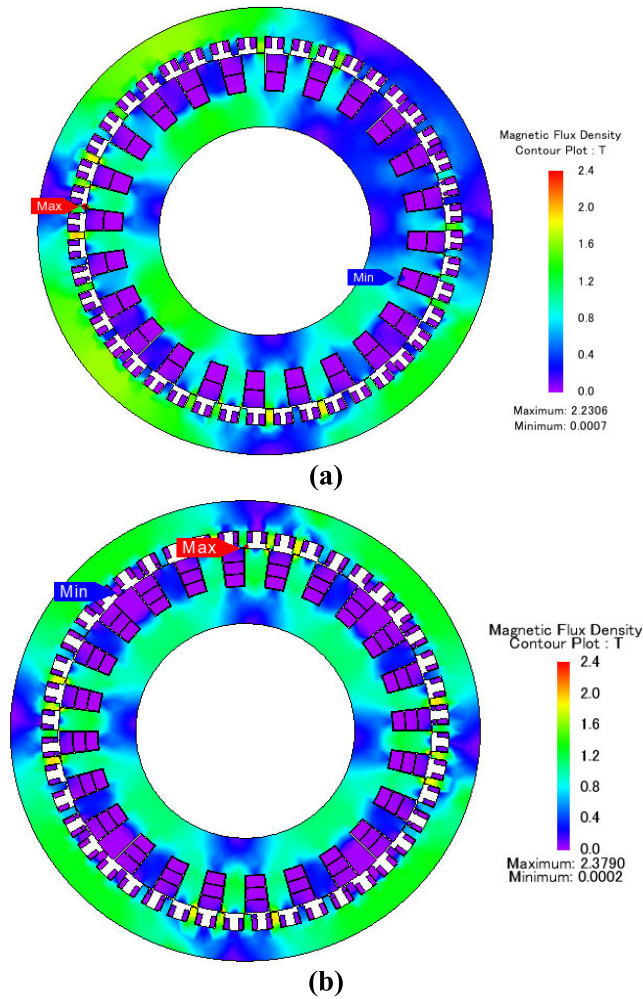


FIGURE 14. Flux density distribution plots of (a) subharmonic BL-WRVM (b) proposed third-harmonic BL-WRVM.

harmonic field excitation. Furthermore, a comparative analysis was done between the conventional and proposed topology under the same operating conditions. The results showed that the rectified field current for the proposed third harmonic model was higher due to an increase in the excitation current as compared to the subharmonic model. Moreover, the third harmonic-based topology generates 10.1% higher torque as compared to the subharmonic model.

The results further conclude that the performance of the proposed self-excited BL-WRVM is better due to pole increment, average output torque, and efficiency. With the utilization of third harmonic, there was a significant increase in torque ripple as compared to subharmonic field excitation that could be minimized by an optimal design of a machine. Nevertheless, the proposed topology is cost-effective as compared to the other brushless wound rotor machine topologies and can be used in automotive industries.

REFERENCES

[1] D. G. Dorrell, "Are wound-rotor synchronous motors suitable for use in high efficiency torque-dense automotive drives?" in *Proc. 38th Annu. Conf. IEEE Ind. Electron. Soc.*, Oct. 2012, pp. 4880–4885, doi: 10.1109/IECON.2012.6389578.

- [2] W. Chai, T. Lipo, and B.-I. Kwon, "Design and optimization of a novel wound field synchronous machine for torque performance enhancement," *Energies*, vol. 11, no. 8, p. 2111, Aug. 2018.
- [3] L. Sun, X. Gao, F. Yao, Q. An, and T. Lipo, "A new type of harmonic current excited brushless synchronous machine based on an open winding pattern," in *Proc. IEEE Energy Convers. Congr. Exposit. (ECCE)*, Sep. 2014, pp. 2366–2373, doi: 10.1109/ECCE.2014.6953719.
- [4] R. D. Hall and R. P. Roberge, "Carbon brush performance on slip rings," in *Proc. Conf. Rec. Annu. Pulp Paper Ind. Tech. Conf.*, Jun. 2010, pp. 1–6, doi: 10.1109/PAPCON.2010.5556522.
- [5] D. Dorrell, L. Parsa, and I. Boldea, "Automotive electric motors, generators, and actuator drive systems with reduced or no permanent magnets and innovative design concepts," *IEEE Trans. Ind. Electron.*, vol. 61, no. 10, pp. 5693–5695, Oct. 2014.
- [6] P. I. Nippes, "Harmonic power in nonsalient-pole synchronous machinery," *Trans. Amer. Inst. Electr. Engineers. III, Power App. Syst.*, vol. 81, no. 3, pp. 419–422, Apr. 1962, doi: 10.1109/AIEEPAS.1962.4501343.
- [7] M. Ayub, S. S. H. Bukhari, G. Jawad, and B.-I. Kwon, "Brushless wound field synchronous machine with third-harmonic field excitation using a single inverter," *Electr. Eng.*, vol. 101, no. 1, pp. 165–173, Apr. 2019.
- [8] F. Yao, D. Sun, L. Sun, and T. A. Lipo, "Dual third-harmonic-current excitation principle of a brushless synchronous machine based on double three-phase armature windings," in *Proc. 22nd Int. Conf. Electr. Mach. Syst. (ICEMS)*, Harbin, China, Aug. 2019, pp. 1–4.
- [9] F. Yao, Q. An, L. Sun, and T. A. Lipo, "Performance investigation of a brushless synchronous machine with additional harmonic field windings," *IEEE Trans. Ind. Electron.*, vol. 63, no. 11, pp. 6756–6766, Nov. 2016, doi: 10.1109/TIE.2016.2581759.
- [10] S. S. H. Bukhari, H. Ahmad, G. J. Sirewal, and J. Ro, "Simplified brushless wound field synchronous machine topology based on a three-phase rectifier," *IEEE Access*, vol. 9, pp. 8637–8648, 2021.
- [11] Q. Ali, T. A. Lipo, and B. Kwon, "Design and analysis of a novel brushless wound rotor synchronous machine," *IEEE Trans. Magn.*, vol. 51, no. 11, pp. 1–4, Nov. 2015, doi: 10.1109/TMAG.2015.2440433.
- [12] G. Jawad, Q. Ali, T. A. Lipo, and B. Kwon, "Novel brushless wound rotor synchronous machine with zero-sequence third-harmonic field excitation," *IEEE Trans. Magn.*, vol. 52, no. 7, pp. 1–4, Jul. 2016.
- [13] C. Lee, "Vernier motor and its design," *IEEE Trans. Power App. Syst.*, vol. PAS-82, no. 66, pp. 343–349, Jun. 1963, doi: 10.1109/TPAS.1963.291362.
- [14] D. K. Jang and J. H. Chang, "Performance comparison of PM synchronous and PM Vernier machines based on equal output power per unit volume," *J. Elect. Eng. Technol.*, vol. 11, no. 1, pp. 150–156, 2016.
- [15] T. M. Pushman, R.-J. Wang, S. Gerber, C. D. Botha, and M. J. Kamper, "Design and performance comparison of Vernier and conventional PM synchronous wind generators," *IEEE Trans. Ind. Appl.*, vol. 56, no. 3, pp. 2570–2579, Mar. 2020.
- [16] Q. Ali, A. Hussain, N. Baloch, and B. Kwon, "Design and optimization of a brushless wound-rotor Vernier machine," *Energies*, vol. 11, no. 2, p. 317, Feb. 2018, doi: 10.3390/EN11020317.
- [17] S. Tariq, J. Ikram, S. S. H. Bukhari, Q. Ali, A. Hussain, and J. Ro, "Design and analysis of single inverter-fed brushless wound rotor Vernier machine," *IEEE Access*, vol. 10, pp. 101609–101621, 2022, doi: 10.1109/ACCESS.2022.3209501.
- [18] S. S. H. Bukhari, G. J. Sirewal, M. Ayub, and J. Ro, "A new small-scale self-excited wound rotor synchronous motor topology," *IEEE Trans. Magn.*, vol. 57, no. 2, pp. 1–5, Feb. 2021.
- [19] S. S. H. Bukhari, J. Ikram, F. Wang, X. Yu, J. Imtiaz, J. Rodas, and J. Ro, "Novel self-excited brush-less wound field Vernier machine topology," *IEEE Access*, vol. 10, pp. 97868–97878, 2022, doi: 10.1109/ACCESS.2022.3206381.
- [20] B. Kim, "Characteristic analysis of a Vernier PM motor considering adjustable speed control," in *Proc. IEEE Transp. Electrification Conf. Expo. Asia-Pacific (ITEC Asia-Pacific)*, Busan, South Korea, Jun. 2016, pp. 671–676.
- [21] I. Ahmad, J. Ikram, M. Yousuf, R. Badar, S. S. H. Bukhari, and J. Ro, "Performance improvement of multi-rotor axial flux Vernier permanent magnet machine by permanent magnet shaping," *IEEE Access*, vol. 9, pp. 143188–143197, 2021, doi: 10.1109/ACCESS.2021.3121271.

...